

# Cancer Research

## Pyrimethamine Induces Apoptosis of Melanoma Cells via a Caspase and Cathepsin Double-Edged Mechanism

Anna Maria Giammarioli, Angela Maselli, Andrea Casagrande, et al.

*Cancer Res* 2008;68:5291-5300.

**Updated version** Access the most recent version of this article at:  
<http://cancerres.aacrjournals.org/content/68/13/5291>

**Supplementary Material** Access the most recent supplemental material at:  
<http://cancerres.aacrjournals.org/content/suppl/2008/06/25/68.13.5291.DC1.html>

**Cited Articles** This article cites by 41 articles, 13 of which you can access for free at:  
<http://cancerres.aacrjournals.org/content/68/13/5291.full.html#ref-list-1>

**Citing articles** This article has been cited by 5 HighWire-hosted articles. Access the articles at:  
<http://cancerres.aacrjournals.org/content/68/13/5291.full.html#related-urls>

**E-mail alerts** [Sign up to receive free email-alerts](#) related to this article or journal.

**Reprints and Subscriptions** To order reprints of this article or to subscribe to the journal, contact the AACR Publications Department at [pubs@aacr.org](mailto:pubs@aacr.org).

**Permissions** To request permission to re-use all or part of this article, contact the AACR Publications Department at [permissions@aacr.org](mailto:permissions@aacr.org).

# Pyrimethamine Induces Apoptosis of Melanoma Cells via a Caspase and Cathepsin Double-Edged Mechanism

Anna Maria Giammarioli,<sup>1</sup> Angela Maselli,<sup>1</sup> Andrea Casagrande,<sup>2</sup> Lucrezia Gambardella,<sup>1</sup> Angelo Gallina,<sup>2</sup> Massimo Spada,<sup>2</sup> Antonello Giovannetti,<sup>3</sup> Enrico Proietti,<sup>2</sup> Walter Malorni,<sup>1</sup> and Marina Pierdominici<sup>2</sup>

<sup>1</sup>Department of Drug Research and Evaluation and <sup>2</sup>Department of Cell Biology and Neurosciences, Istituto Superiore di Sanità; <sup>3</sup>Department of Clinical Medicine, Division of Clinical Immunology, University of Rome "La Sapienza," Rome, Italy

## Abstract

The unresponsiveness of metastatic melanoma to conventional chemotherapeutic and biological agents is largely due to the development of resistance to apoptosis. Pyrimethamine belongs to the group of antifolate drugs, and in addition to antiprotozoan effects, it exerts a strong proapoptotic activity, which we recently characterized in human T lymphocytes. However, no data regarding pyrimethamine anticancer activity are available thus far. To this end, we examined the *in vitro* effects of pyrimethamine on apoptosis, cell cycle distribution, and cell proliferation of human metastatic melanoma cell lines. The *in vivo* antitumor potential of pyrimethamine was evaluated in a severe combined immunodeficiency (SCID) mouse xenotransplantation model. Our data indicate that pyrimethamine, when used at a clinically relevant concentration, induced apoptosis in metastatic melanoma cells via the activation of the cathepsin B and the caspase cascade (i.e., caspase-8 and caspase-9) and subsequent mitochondrial depolarization. This occurred independently from CD95/Fas engagement. Moreover, pyrimethamine induced a marked inhibition of cell growth and an S-phase cell cycle arrest. Results obtained in SCID mice, injected s.c. with metastatic melanoma cells and treated with pyrimethamine, indicated a significant inhibitory effect on tumor growth. In conclusion, our results suggest that pyrimethamine-induced apoptosis may be considered as a multifaceted process, in which different inducers or regulators of apoptosis are simultaneously implicated, thus permitting death defects of melanoma cells to be bypassed or overcome. On these bases, we hypothesize that pyrimethamine could represent an interesting candidate for the treatment of metastatic melanoma. [Cancer Res 2008;68(13):5291–300]

## Introduction

The incidence and mortality rate of malignant melanoma is continuously increasing worldwide (1). Metastatic melanoma has a poor prognosis, as it is largely resistant to conventional chemotherapeutic and biological agents (2). In monotherapy regimens, dacarbazine is still considered the standard first-line

treatment, although it rarely leads to complete remission (5–10% of patients; ref. 3). Several other chemotherapeutic agents (fotemustine, vindesine, and temozolomide) have a similar activity to dacarbazine, but none of these drugs has been shown to significantly increase the overall survival of melanoma patients. Combined treatment schedules (polychemotherapy, combinations of cytostatic drugs and cytokines) are able to increase response rates up to 20% to 40% (3, 4). However, none of these combined treatment regimens has been shown to significantly prolong survival in randomized studies.

Despite a range of different biochemical targets, available agents generally kill cancer cells by induction of apoptosis. Melanoma cells have low levels of spontaneous apoptosis *in vivo* compared with other tumor cell types and are relatively resistant to drug-induced apoptosis *in vitro* (5, 6).

Traditionally, two main cell death pathways have been recognized: the mitochondrial and the death receptor pathways, which involve caspase-9, caspase-2, and caspase-8, caspase-10, respectively (7). However, both pathways converge toward specific mitochondrial changes. In particular, alterations of mitochondrial membrane potential ( $\Delta\psi$ ) are associated with the release of apoptogenic factors, e.g., the release of cytochrome *c*, the apoptosome formation, and, finally, the chromatin clumping and DNA fragmentation. In addition to caspase-mediated proteolysis, other proteases, such as cathepsins, may also be involved in the regulation of apoptosis (8). Cathepsins are released from their physiologic compartment, i.e., the lysosome, and trigger apoptotic cell death via various pathways, including the activation of caspases or the release of proapoptotic factors from the mitochondria. Cathepsin-mediated cell death has been associated with metastatic melanoma since 1986 (9), and we recently showed that this enzymatic cascade was capable of apoptotic induction in cisplatin-treated melanoma cell lines (10).

Pyrimethamine (2,4-diamino-5-p-chlorophenyl-6-ethyl-pyrimidine) belongs to the group of antifolate drugs blocking the enzyme dihydrofolate reductase, which is essential for the synthesis of folic acid, a cofactor required for DNA synthesis. It is used in the treatment of infections caused by protozoan parasites, such as *Toxoplasma gondii* and *Plasmodium falciparum* (11). In addition to its antiprotozoal effects, pyrimethamine may exert immunomodulating activities, including the induction of peripheral blood lymphocyte apoptosis (12–15). We showed that this drug induces apoptosis of activated lymphocytes via a mechanism that brings into play the upstream caspases (16). However, although the primary target of pyrimethamine is represented by the caspase-8-driven cascade, this drug also acts on mitochondria. In fact, similar to other antifolate compounds, pyrimethamine leads to mitochondrial membrane depolarization, which is a late event in the

Note: Supplementary data for this article are available at Cancer Research Online (<http://cancerres.aacrjournals.org/>).

W. Malorni and M. Pierdominici are to be considered as senior authors.

Requests for reprints: Walter Malorni, Department of Drug Research and Evaluation, Section of Cell Aging and Degeneration, Istituto Superiore di Sanità, viale Regina Elena 299, 00161, Rome, Italy. Phone: 39-6-49902905; Fax 39-6-49903691; E-mail: malorni@iss.it.

©2008 American Association for Cancer Research.  
doi:10.1158/0008-5472.CAN-08-0222

mitochondrially driven apoptotic cascade (17). It is interesting to consider that the expression of Bcl-2 (a regulator of mitochondrial proapoptotic activity) is down-regulated by pyrimethamine in peripheral blood lymphocytes.

No data on anticancer potential of pyrimethamine are presently available. The aim of the present study was to evaluate the *in vitro* and *in vivo* antitumor activity of pyrimethamine in human metastatic melanoma cells. To this end, we examined the *in vitro* effects of pyrimethamine on cell proliferation, cell cycle distribution, and apoptosis of human metastatic melanoma cells. The *in vivo* antitumor potential of pyrimethamine was also evaluated in a severe combined immunodeficiency (SCID)-mouse xenotransplantation model.

## Materials and Methods

### Cell Lines

Human metastatic melanoma cell lines 8863 and 501 have been previously described (10, 18). These cell lines were cultured in RPMI 1640 (Life Technologies, Invitrogen) supplemented with 10% heat-inactivated fetal bovine serum (Euroclone), 2 mmol/L glutamine (Sigma), and 50 µg/mL gentamicin (Sigma). Tumor cells were tested as *Mycoplasma*-free (*Mycoplasma* detection kit; Roche).

### Culture Conditions and Analysis of Cell Viability

Pyrimethamine (Sigma) and temozolomide (Sigma) were dissolved in DMSO and diluted in RPMI 1640 immediately before experiments. Melanoma cells were exposed for 24, 48, and 72 h to (a) pyrimethamine (0.32, 32, and 320 µmol/L) and (b) temozolomide (100 µmol/L). To activate the CD95/Fas pathway, an antihuman Fas IgM monoclonal antibody (mAb) was added to melanoma cells (clone CH11, 500 ng/mL; Upstate Biotechnology). Pyrimethamine treatment was also performed in cells pretreated with (a) neutralizing antihuman Fas IgG1 (clone ZB4, 10 µg/mL; Upstate Biotechnology), (b) cathepsin B inhibitor (CA-074-Me, 10 µmol/L; Calbiochem), and (c) pan-caspase inhibitor z-VAD-fmk (50 µmol/L; R&D Systems). Time-dependent inhibition of cell growth and survival was determined using trypan blue exclusion method.

### Analytic Cytology Analyses

**Surface phenotyping and Bcl-2 expression.** Surface phenotyping and Bcl-2 expression analyses were performed by flow cytometry, as described before (16). The following mAbs were used: anti-CD95 conjugated to FITC (BD Immunocytometry Systems) and anti-Bcl-2-FITC (DAKO).

**Evaluation of apoptosis.** Quantitative evaluation of apoptosis was performed by a double staining flow cytometry method using FITC-conjugated Annexin V (AV)/propidium iodide (PI) apoptosis detection kit (Marine Biological Laboratory) according to the manufacturer's protocol. Reported data are referred to both early (AV<sup>+</sup>/PI<sup>-</sup> cells, still alive) and late (AV<sup>+</sup>/PI<sup>+</sup> cells, dead cells) apoptotic melanoma cells.

**Mitochondrial membrane potential ( $\Delta\Psi$ ).**  $\Delta\Psi$  was studied by using the lipophilic cationic probe 5'-5',6'-6'-tetrachloro-1,1',3,3'-tetraethylbenzimidazol-carbocyanine iodide (JC-1; Molecular Probes), as previously described (19).

**Measurement of cathepsin B.** The expression and the activation state of cathepsin B was evaluated by both flow cytometry and Western blot, as previously described (10). For details, see Supplementary Materials and Methods.

**Caspase activity.** Caspase-8 and caspase-9 activities were assayed by using the CaspGLOW fluorescein active caspase staining kit (MBL), following the manufacturer's instruction, as previously described (16). Western blot was also performed as described before (10). For details, see Supplementary Materials and Methods.

**Cell cycle analysis.** Cultured cells were treated with 1 mmol/L bromodeoxyuridine (BrdUrd; BD Immunocytometry Systems) for 30 min, removed from culture, and fixed in 70% ice-cold ethanol.  $1 \times 10^6$  fixed cells were incubated in 3N HCl for 20 min. After washing with 0.1 mol/L

Na<sub>2</sub>B<sub>4</sub>O<sub>7</sub> (pH 8.5) to stop acid denaturation, cells were washed twice with 1% bovine serum albumin and 0.5% Tween 20 and labeled with an anti-BrdUrd FITC-conjugated mAb (BD Immunocytometry Systems) for 30 min at 4°C. Cells were then stained with 40 µg/mL PI (Sigma) in the presence of 10 µmol/L RNase (Sigma) for 30 min at 37°C followed by analysis on a flow cytometer.

**Static cytometry analysis.** To visualize intracellular distribution of cathepsin B and filamentous actin (F-actin), static cytometry analysis was performed as previously described (10). For details, see Supplementary Materials and Methods.

**ELISA.** To evaluate cytochrome *c* release from mitochondria, the total cell suspension was centrifuged and washed in ice-cold PBS and the cytosolic fraction was separated by means of the cytochrome *c* releasing apoptosis assay kit (Biovision), as previously described (20). Protein content was determined by the Bradford assay (Bio-Rad). The amount of cytosolic cytochrome *c* in the cytosolic fraction was quantified by using a commercially available ELISA kit following the instructions from the manufacturer (R&D Systems).

### Animals

CB.17 SCID/SCID female mice (Harlan Italy) were used at 4 to 5 wk of age and were kept under specific pathogen-free conditions. SCID mice were housed in filter top cages and were provided with sterile water and food *ad libitum*. All manipulations were carried out aseptically inside a laminar flow hood. Before injection of the melanoma cells, mice were weighed and grouped (adjusted to a mean body weight of 20 g, range 18.5–21.0 g) into two treatment groups and two control groups (eight mice per group). The cell system used was represented by the human melanoma cell line 501, derived from a metastatic tumor lesion (18), cultured as reported above. For injection, *Mycoplasma*-free melanoma cells were harvested by trypsinization, tested for viability (>95%), and adjusted to a concentration of  $1 \times 10^7$  viable cells per 1 mL medium. Mice were injected s.c. into the right flank with  $2 \times 10^6$  501 cells per mouse. Suspensions of pyrimethamine were prepared daily in citrate buffer of 200 mmol/L 0.5% methylcellulose.

At the onset of tumor (i.e., 7 d from melanoma cell injection), mice were given by oral gavage with the same volume (400 µL) of vehicle or pyrimethamine at different doses (3, 6, 30, and 60 mg/kg) 5 d a week up to 42 d from injection (30 d of pyrimethamine treatment). An untreated control group was also included. All mice were inspected daily, and the overall clinical condition was assessed. Tumor growth was monitored by measuring maximal and minimal diameters by caliper, and tumor weight was estimated with the formula: tumor weight (mg) = [length (mm) × width<sup>2</sup> (mm)] / 2, as previously described (18, 21). Procedures and facilities followed the requirements of Commission Directive 86/609/EEC concerning the protection of animals used for experimental and other scientific purposes. Italian legislation is defined in D.L. no. 116 of January 27, 1992.

### Immunohistochemistry

After 42 d of tumor growth, mice were sacrificed and the primary melanoma was removed by excision and fixed in 10% buffered formalin before being embedded in paraffin. Paraffin-embedded tissues were serially sectioned, dried at 80°C for 60 min, and deparaffinized according to routine procedures. Sections were then incubated in citrate buffer (pH 6.0) and microwaved for 15 min.

**Morphometric analysis.** For cell proliferation analysis, tissue sections were incubated with mouse anti-human Ki-67 antibody (clone MIB-1; DAKO) followed by the application of a biotinylated secondary antibody. Apoptosis was evaluated by terminal deoxyribonucleotidyl transferase-mediated dUTP nick end labeling staining (TUNEL) by using the DeadEnd kit (Promega). The slides were observed with a Nikon Optiphot microscope (Nikon). Both proliferating and apoptotic cells were quantified by analyzing 20 different microscope fields at the same magnification (200×).

### Data Analysis and Statistics

Flow cytometric analyses were performed by using a FACSCalibur flow cytometer (BD Immunocytometry Systems) using the Cell Quest Pro software. Statistical analysis was performed by Student's *t* test using Statview program for Windows.

## Results

**Pyrimethamine induces apoptosis of human metastatic melanoma cells.** We first evaluated the apoptosis-inducing potential of pyrimethamine by treating two metastatic melanoma cell lines (8863 and 501) with different pyrimethamine concentrations for 48 h (Fig. 1A, *left* and *right* for 8863 and 501 cells, respectively). In both cell lines, the proapoptotic effect of pyrimethamine was already remarkable (2.1-fold and 3-fold increase for 8863 and 501 cell lines, respectively) at a concentration of 32  $\mu\text{mol/L}$  corresponding to that detected at the steady-state *in vivo* (22). A 10-fold increase of pyrimethamine concentration did not result in higher apoptosis levels in the 8863 cell line, whereas it further increased cell death in the 501 cell line, reaching values close to 70% to 80%. For all tested concentrations, the percentage of AV<sup>-</sup> cells and PI<sup>+</sup> cells was  $\leq 5\%$ . Control experiments carried out with DMSO alone did not display any proapoptotic activity ( $<10\%$ ). On this basis, we selected the dose of 32  $\mu\text{mol/L}$  as optimal

pyrimethamine concentration for further studies on melanoma cells. To better evaluate pyrimethamine-induced cell death, a time-dependent analysis of apoptosis was also carried out. We cultured melanoma cells in the presence of pyrimethamine at different time points (24, 48, and 72 h). A significant increase of pyrimethamine-induced apoptosis was already detected at 24 h, reaching a plateau value at 72 h in both 8863 (Fig. 1B, *left*) and 501 (Fig. 1B, *right*) cell lines. Also in this case, the percentage of AV<sup>-</sup>/PI<sup>+</sup> cells was  $\leq 5\%$  at all time points analyzed. We focused our attention on the 48 h of pyrimethamine treatment. As a control, to better evaluate the therapeutic potential of pyrimethamine, we also assessed the apoptotic susceptibility of our melanoma cells to a typical anticancer drug. To this aim, we treated melanoma cells with temozolomide, a promising chemotherapeutic agent for malignant melanoma (23). We found that both melanoma cell lines analyzed here were resistant to this drug, i.e., no significant apoptosis was detected by using temozolomide at a clinically relevant concentration (100  $\mu\text{mol/L}$ ; ref. 24), at all time points studied (Supplementary

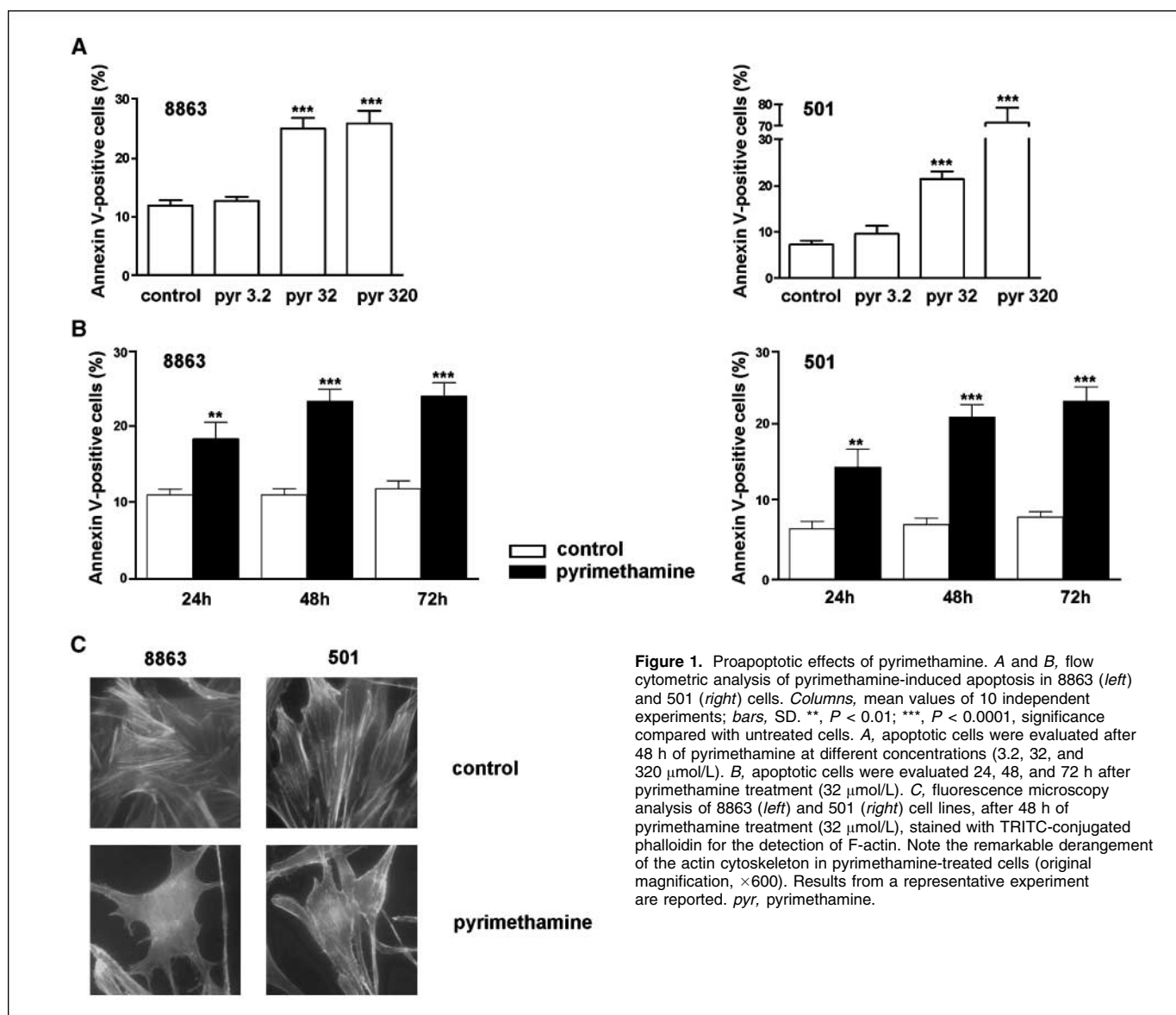


**Figure 1.** Proapoptotic effects of pyrimethamine. *A* and *B*, flow cytometric analysis of pyrimethamine-induced apoptosis in 8863 (*left*) and 501 (*right*) cells. *Columns*, mean values of 10 independent experiments; *bars*, SD. \*\*,  $P < 0.01$ ; \*\*\*,  $P < 0.0001$ , significance compared with untreated cells. *A*, apoptotic cells were evaluated after 48 h of pyrimethamine at different concentrations (3.2, 32, and 320  $\mu\text{mol/L}$ ). *B*, apoptotic cells were evaluated 24, 48, and 72 h after pyrimethamine treatment (32  $\mu\text{mol/L}$ ). *C*, fluorescence microscopy analysis of 8863 (*left*) and 501 (*right*) cell lines, after 48 h of pyrimethamine treatment (32  $\mu\text{mol/L}$ ), stained with TRITC-conjugated phalloidin for the detection of F-actin. Note the remarkable derangement of the actin cytoskeleton in pyrimethamine-treated cells (original magnification,  $\times 600$ ). Results from a representative experiment are reported. *pyr*, pyrimethamine.

Fig. S1). As an active role of the CD95/CD95FasL system in apoptosis induced by antifolate drugs, e.g., methotrexate, was previously shown (25), we also evaluated the expression of CD95/Fas molecule at the cell surface of 8863 and 501 cell lines. A different surface expression of CD95/Fas molecule characterized the two metastatic melanoma cells. In fact, whereas the 8863 cell line showed a weak surface expression of CD95/Fas ( $0.6 \pm 0.3\%$ ; median fluorescence intensity,  $17 \pm 5$ ), the 501 cell line revealed a high expression of CD95/Fas ( $91 \pm 10\%$ ; median fluorescence intensity,  $17 \pm 4$ ). However, both cell lines were resistant to CD95/Fas-induced apoptosis *in vitro* when stimulated with an antihuman Fas IgM monoclonal antibody (clone CH11). In the presence of pyrimethamine, neither the percentage nor the median fluorescence intensity of CD95/Fas molecule changed compared with untreated cells. Furthermore, melanoma cells were treated with the ZB4 mAb, i.e., the CD95 neutralizing antibody, to exclude a direct involvement of CD95/Fas receptor in pyrimethamine-induced apoptosis. The percentage of apoptosis in pyrimethamine-treated melanoma cells remained substantially unchanged in the presence of ZB4 (Supplementary Fig. S2), thus suggesting that the pyrimethamine-induced apoptosis did not involve the CD95/Fas molecule.

In this set of experiments, aimed at evaluating the apoptosis-inducing potential of pyrimethamine, the expression of a key molecule in the inhibition of apoptotic cell death pathway (i.e., the Bcl-2 molecule) was also assessed. A down-regulation of Bcl-2 expression was detected after treatment with pyrimethamine in both cell lines. In fact, compared with control cells, Bcl-2 expression decreased  $27 \pm 5\%$  in 8863 and  $59 \pm 8\%$  in 501 cell lines.

Finally, as cytoskeletal molecules are well known to be involved in some important tumor processes, such as migration and invasion (26), a morphologic analysis of actin filament network in pyrimethamine-treated 8863 and 501 cell lines was performed. As compared with untreated cells, a breakdown of the F-actin filaments was detected (Fig. 1C, *left* and *right* for 8863 and 501 cell lines, respectively).

**Pyrimethamine induces cathepsin B-dependent and caspase-dependent apoptosis in melanoma cells.** To identify the apoptotic pathway being activated in response to pyrimethamine (i.e., caspase and/or cathepsin pathway), 8863 and 501 cell lines were initially pretreated with the pan-caspase inhibitor Z-VAD-FMK and/or the cathepsin B inhibitor CA-074-Me. We evaluated pyrimethamine-induced apoptosis at 24, 48, and 72 h of culture (Fig. 2). In the 8863 cell line, Z-VAD-FMK significantly inhibited pyrimethamine-induced apoptosis after 72 h of treatment (Fig. 2A;  $P = 0.0033$ ). In the 501 cell line, a minor protective effect was exerted by Z-VAD-FMK (Fig. 2B) at all times of pyrimethamine treatment. When the cathepsin B inhibitor (CA-074-Me) was used, pyrimethamine-induced apoptosis was significantly abrogated in the 8863 cell line after 24 h (Fig. 2A;  $P = 0.0376$ ). This effect persisted, although at a minor extent, after 48 h ( $P = 0.0279$ ) and was lost after 72 h of pyrimethamine addition. Differently, only a partial protection from pyrimethamine-induced apoptosis was exerted by the cathepsin B inhibitor in the 501 cell line at each time point studied (Fig. 2B). Notably, when the two inhibitors (i.e., caspase and cathepsin B inhibitors) were used in combination, a complete protection was obtained in both the 8863 and 501 cell lines at all time points.

The possible involvement of upstream caspases (i.e., caspase-8 mainly involved in receptor-mediated apoptosis and caspase-9 mainly involved in mitochondria-mediated apoptosis) and/or cathepsin B was evaluated by both flow cytometric and Western blot analyses. In the 8863 cell line, flow cytometric data showed an increased expression of intracellular cathepsin B 24 h after pyrimethamine addition, which persisted at later time points (Fig. 3A, *right*). The activation of caspase-9, but not of caspase-8, was also detected after 48 and 72 h of pyrimethamine addition (Fig. 3A, *middle* and *left*, respectively). Western Blot analysis confirmed these results, showing an early activation of cathepsin B and a later activation of caspase-9 (Fig. 3B). Similarly to what was observed in the 8863 cell line, cathepsin B expression increased in the 501 cell line, starting from 24 h of pyrimethamine treatment (Fig. 3A, *right*).

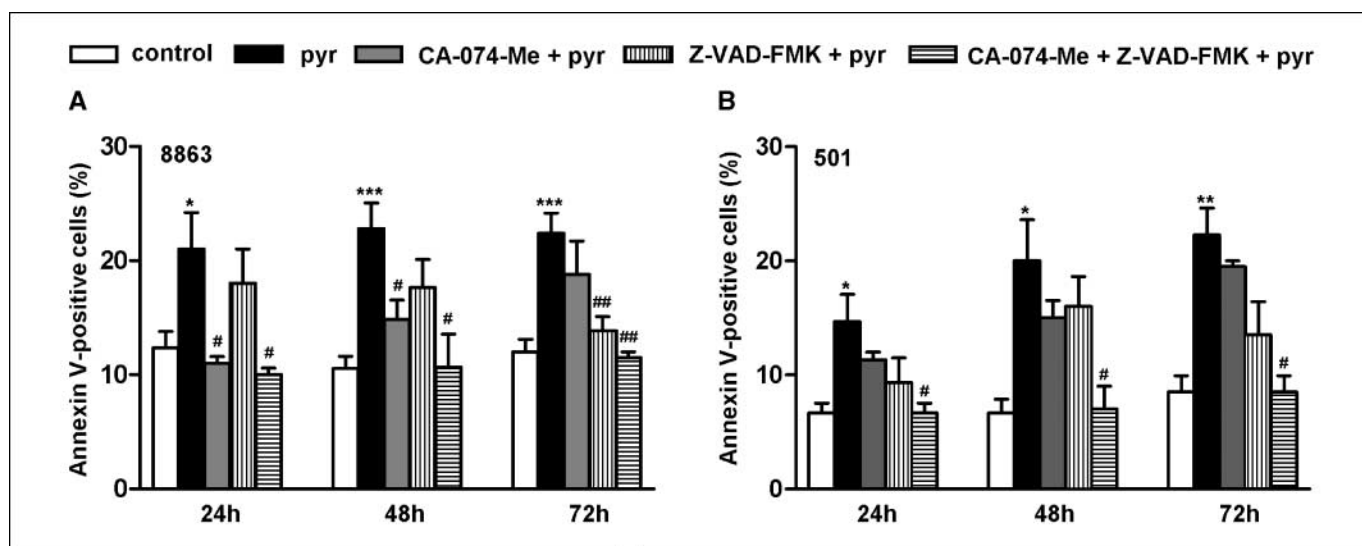


**Figure 2.** Pyrimethamine-induced apoptosis in 8863 (A) and 501 (B) cells pretreated with the pan caspase inhibitor Z-VAD-FMK and/or the cathepsin B inhibitor CA-074-Me. The percentage of apoptotic cells was evaluated after 24, 48, and 72 h of pyrimethamine treatment in both 8863 and 501 cell lines pretreated for 4 h with the pan caspase inhibitor z-VAD-fmk ( $50 \mu\text{mol/L}$ ) and/or the cathepsin B inhibitor CA-074-Me ( $10 \mu\text{mol/L}$ ). Columns, mean values of three independent experiments; bars, SD. \*,  $P < 0.05$ ; \*\*,  $P < 0.01$ ; \*\*\*,  $P < 0.0001$ , significance compared with untreated cells. #,  $P < 0.05$ ; ##,  $P \leq 0.01$ , significance compared with pyrimethamine-treated cells.

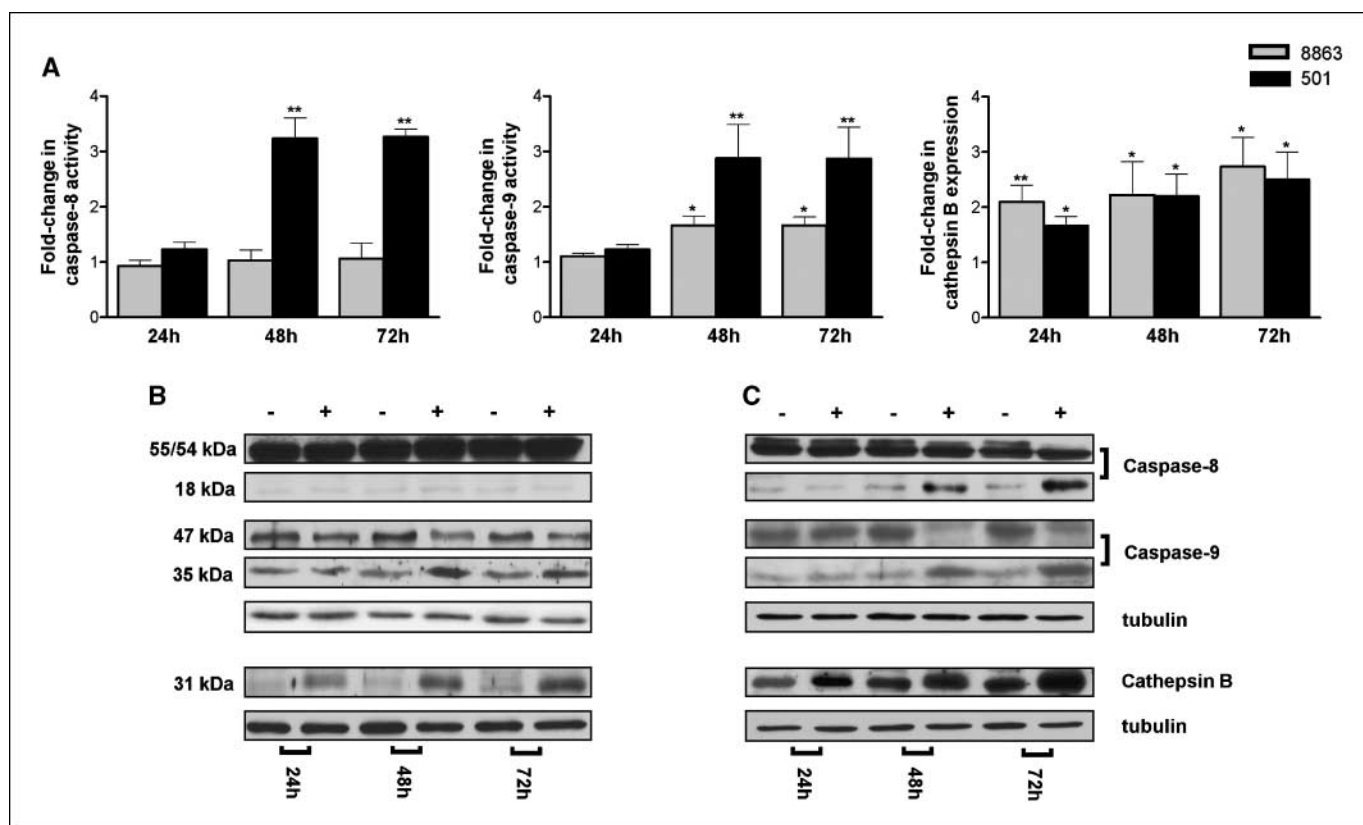


**Figure 3.** Flow cytometric (A) and Western blot analyses (B and C) of cathepsin B and caspase-8 and caspase-9 in pyrimethamine-treated 8863 and 501 cell lines. A, caspase-8 (left) and caspase-9 (middle) activity and cathepsin B (right) expression were measured by flow cytometry. Results are expressed as the fold increase in pyrimethamine-treated cells over that of untreated cells. Columns, mean values of three independent experiments; bars, SD. \*,  $P < 0.05$ ; \*\*,  $P < 0.01$ , significance compared with untreated cells. B and C, caspase-8, caspase-9, and cathepsin B activity in pyrimethamine-treated 8863 (B) and 501 (C) cell lines measured by Western Blot analysis. Cleaved cathepsin B (31 kDa) and caspase-9 (35 kDa) were detected after 24 and 48 h of pyrimethamine treatment, respectively, in both 8863 and 501 cell lines. In the 501 cell line, but not in the 8863, cleaved caspase-8 (18 kDa) was also observed. Results obtained from a representative experiment are reported.

In this cell line, the activation of both caspase-8 and caspase-9 was also detected after 48 and 72 h of pyrimethamine addition (Fig. 3A, middle and left, respectively). Also in this case, Western Blot analysis confirmed the results obtained by flow cytometry showing an early involvement of cathepsin B and a later activation of both caspase-8 and caspase-9 (Fig. 3C). Taken together, these results suggest a key role for cathepsin B as an early inducer of pyrimethamine-induced apoptosis, whereas the contribution of caspases was detected later in both 501 and 8863 cell lines.

As cathepsin B has been characterized and identified as a native protein for assessing lysosomal integrity during apoptosis (27), we also analyzed cathepsin B localization in our melanoma cell lines before and after pyrimethamine addition. To visualize lysosomes, cells were loaded with LysoTracker Red, a fluorescent dye that predominantly loads into lysosomes (see Materials and Methods). As shown in Fig. 4A, untreated 8863 cells displayed a yellow punctate pattern resulting from the overlap of green and red fluorescence and consistent with cathepsin B (green fluorescence) colocalization to the lysosome vesicular compartment (red fluorescence), at all time points studied. After pyrimethamine treatment, cathepsin B exhibited a more diffuse green fluorescent staining that corresponded to the release of the enzyme from lysosomes to the cytosol. Similarly, 501 cell line displayed yellow punctate areas in untreated cells and a diffuse green fluorescence starting from 24 h of pyrimethamine addition (Fig. 4B).

**Pyrimethamine induces mitochondrial modifications.** To further characterize the apoptotic pathway triggered by pyrimethamine in melanoma cells, we also focused on the possible role of mitochondria, which are well-known regulators of cell death (28). In particular, previous studies suggested that significant reduction in  $\Delta\psi$  and cytochrome *c* release from mitochondria into the cytosol are hallmarks of apoptosis-associated mitochondrial modifications (29, 30). Therefore, time-dependent changes occurring in  $\Delta\psi$  and the release of cytochrome *c* were analyzed. Pyrimethamine induced mitochondrial depolarization at all time points studied in both cell lines (Supplementary Fig. S3). Parallel analyses carried out on cytosolic cytochrome *c* clearly indicated a significant release of this apoptogenic factor starting from 24 h of pyrimethamine treatment in both cell lines (Supplementary Table S1).

**Pyrimethamine causes growth inhibition in human metastatic melanoma cell lines.** To better define the therapeutic potential of pyrimethamine in the treatment of melanoma, the antiproliferative activity of the drug in the two melanoma cell lines was also evaluated. Cells were incubated with 32  $\mu\text{mol/L}$  pyrimethamine, and cell growth was evaluated in terms of viable cell counts after 24, 48, and 72 h of culture. As illustrated in Fig. 5A and B, pyrimethamine caused a time-dependent growth inhibition in both cell lines. This effect was already detectable after 24 h of culture (21% of inhibition in both cell lines) and gradually rose

reaching values of ~70% and 80% of cell growth inhibition at 72 h in 8863 and 501 cell lines, respectively.

**Pyrimethamine induces S-phase cell cycle arrest of human metastatic melanoma cell lines.** To further investigate the mechanism underlying cell growth inhibition induced by pyri-

methamine, 8863 and 501 cell lines were exposed to the drug and then analyzed for cell cycle distribution. Subconfluent cell cultures were treated with pyrimethamine at the same concentration used in the above-mentioned apoptosis assays (32  $\mu\text{mol/L}$ ) and harvested after 48 h of culture. In Fig. 5C, representative plots of

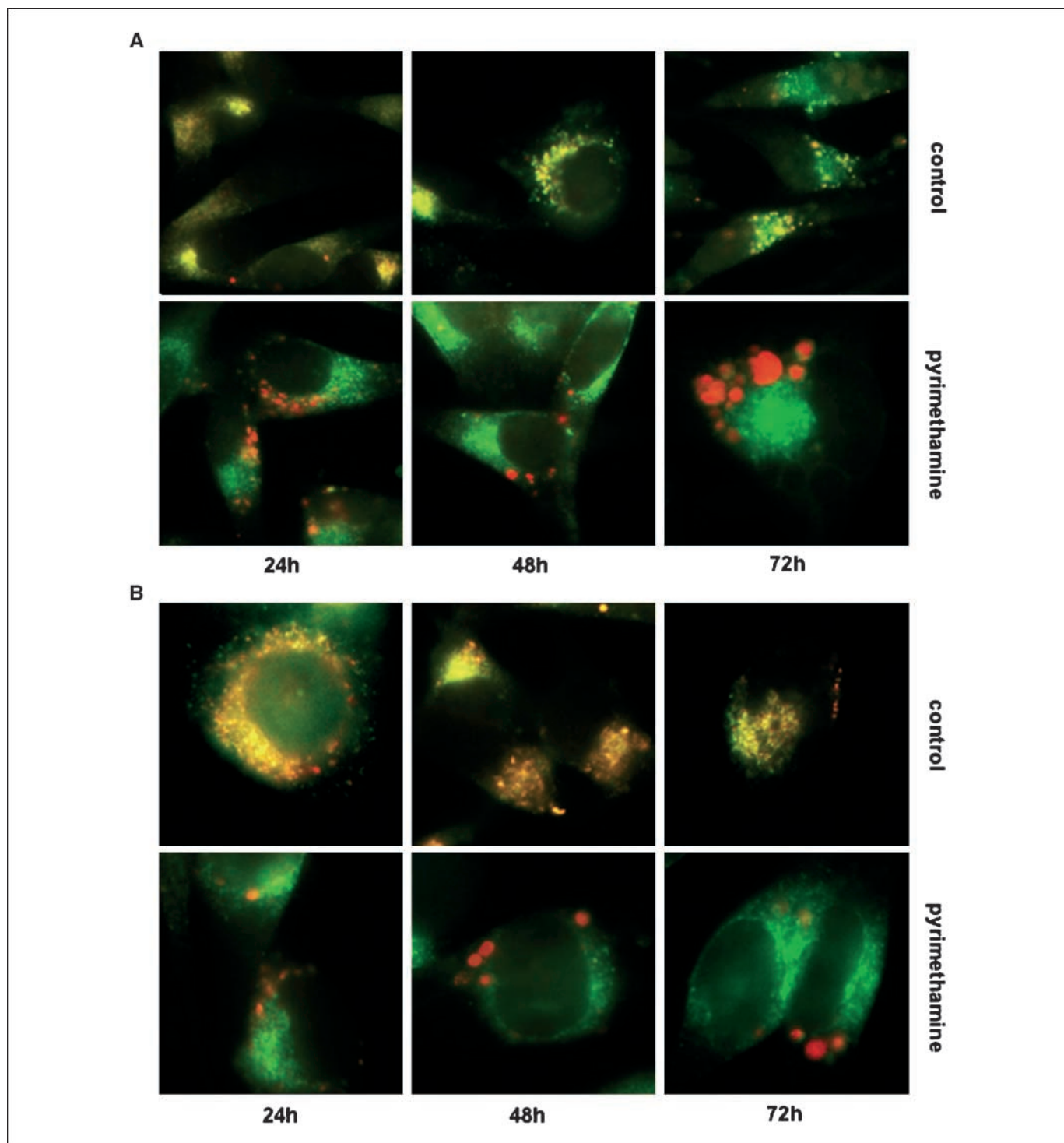


**Figure 4.** Time course analysis of the release of cathepsin B from lysosomes as detected by immunofluorescence microscopy (original magnification, 600 $\times$ ). Representative results obtained with 8863 (A) and 501 (B) cell lines are reported. Lysosomes were stained with Lysotracker Red and the cathepsin B with green fluorescent antibody. A yellow punctate pattern, resulting from the overlay of green and red fluorescence, was consistent with cathepsin B localization to the lysosome vesicular compartment. Note instead green fluorescence, indicating cathepsin B release from lysosomes, in pyrimethamine-treated cells.

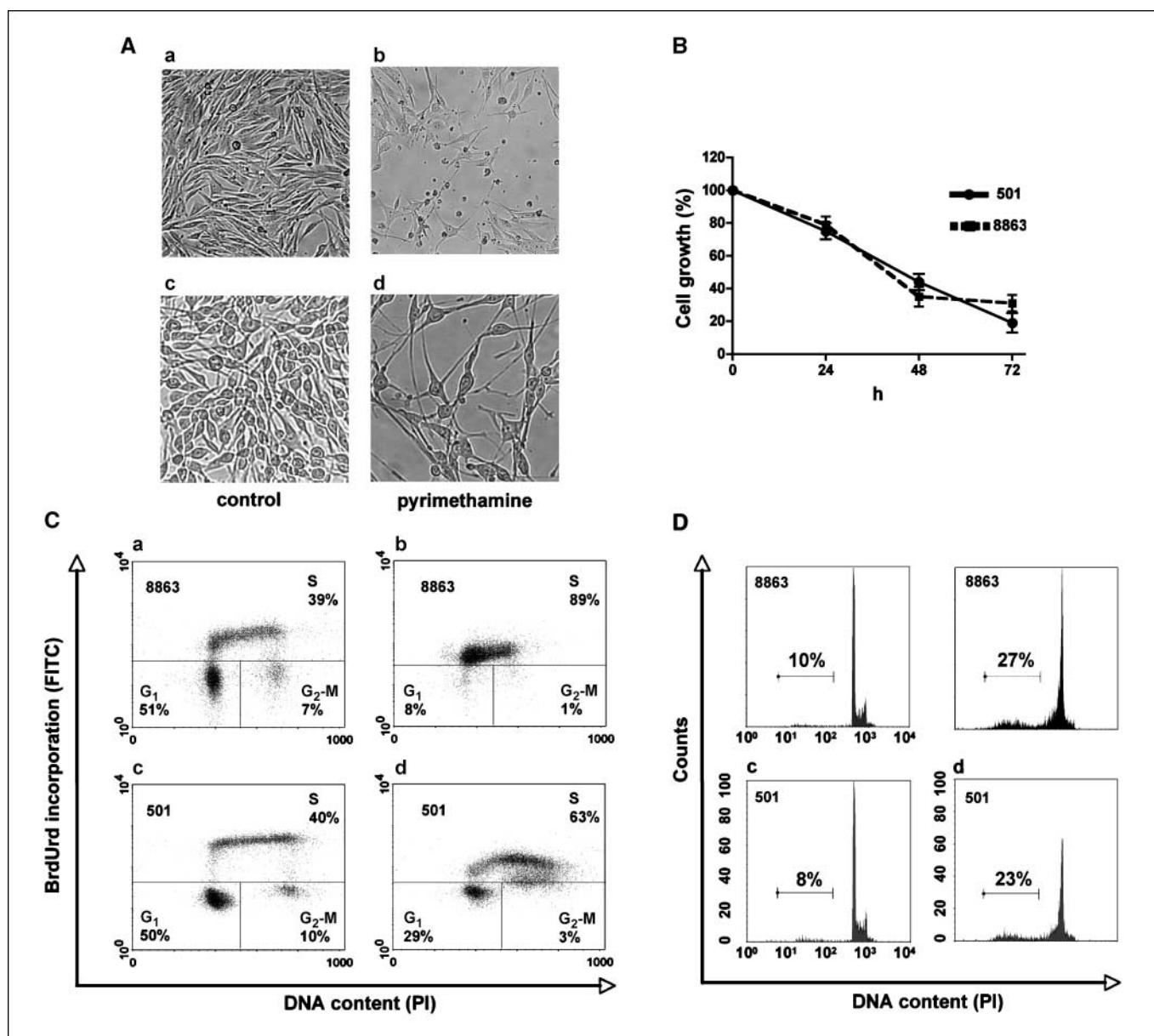


**Figure 5.** Growth inhibition, cell cycle analysis, and DNA fragmentation of 8863 and 501 cell lines after pyrimethamine treatment. *A*, 8863 (*a* and *b*) and 501 (*c* and *d*) cell lines examined by light microscopy (original magnification, 400 $\times$ ) after 48 h pyrimethamine treatment. The data of a representative experiment are shown. *B*, cell growth was calculated in terms of viable cell counts after 24, 48, and 72 h of culture. Data are expressed as the percentage of cell growth with respect to controls. *C*, cell cycle analysis performed by flow cytometry. Representative quadrant plot graphs from three independent experiments are shown. 8863 (*a* and *b*) and 501 (*c* and *d*) cells were cultured in medium alone (*a* and *c*) or in the presence (*b* and *d*) of pyrimethamine for 48 h. Numbers indicate the percentage of viable cells in each phase of the cell cycle. Note that treatment with pyrimethamine induced S-phase arrest in both cell lines. *D*, for each experimental condition shown in *C*, the percentage of cells with fragmented DNA was also evaluated. Apoptotic cells were characterized by a hypodiploid DNA fluorescent pattern (sub-G<sub>1</sub> peak).

BrdUrd versus PI are shown (*a* and *b*, 8863; *c* and *d*, 501). In both cell lines, pyrimethamine induced an increased percentage of cells in the S-phase and a corresponding decrease of cells in the G<sub>1</sub> and G<sub>2</sub>-M phases. At the same time, pyrimethamine induced the formation of a hypodiploid sub-G<sub>1</sub> peak indicative of apoptosis (Fig. 5D). These data suggest that both these mechanisms (i.e., cell cycle arrest and cell loss due to apoptosis) could be responsible for pyrimethamine antiproliferative effects.

**Pyrimethamine reduces melanoma growth in an SCID mouse model.** The *in vivo* efficacy of pyrimethamine was examined by measuring the reduction of tumor growth in a

human melanoma xenograft SCID mouse model. The cell system used was represented by the human metastatic melanoma cell line 501. Pyrimethamine administration started at day 7 post s.c. injection of melanoma cells. The doses of pyrimethamine used to treat mice in this study were chosen on the basis of the highest doses (30 and 60 mg/kg/d) tested in the rat model (31). The doses of 30 and 60 mg/kg/d correspond to a plasma pyrimethamine concentration of 160 and 320  $\mu$ mol/L, respectively (22). Tumor growth and pyrimethamine treatment had no effect on vitality and behavioral responses of animals at the pyrimethamine doses used. No weight loss was observed neither during nor at the end

of the experiment. Vehicle had no effect on tumor growth. A significant reduction of tumor growth ( $P < 0.05$ ) was evident with the dose of 60 mg/kg/d starting from the 22nd day of the injection and up to the end of the experiment (Fig. 6A). Initial experiments performed with lower doses of pyrimethamine (i.e., 3 and 6 mg/kg/d) failed to reveal any effect on tumor growth (data not shown).

**In vivo effects of pyrimethamine on proliferation and apoptosis.** The level of cell proliferation was measured by determining the expression of Ki-67 antigen (a nuclear antigen present only in the nuclei of cycling cells) on tissue sections derived from the tumor grown in SCID mice (excised at day 42 of treatment) and treated or not with pyrimethamine (60 mg/kg/d). Pyrimethamine significantly reduced the percentage of Ki-67-positive 501 cells ( $22 \pm 7\%$ ) compared with controls ( $49 \pm 12\%$ ;  $P = 0.0002$ ; Fig. 6B). TUNEL staining was performed to assess apoptotic rate (Fig. 6C). We found that  $52 \pm 7\%$  of tumor cells were TUNEL positive in sections from mice treated with pyrimethamine, whereas only  $11 \pm 8\%$  of tumor cells were TUNEL positive in sections from control animals ( $P = 0.003$ ). These data suggest that pyrimethamine exerted both antiproliferative and proapoptotic activities, similar to what have been observed in *in vitro* experiments.

## Discussion

In the present work, we characterized the *in vitro* antitumor activity exerted by pyrimethamine in human metastatic melanoma cell lines. The *in vivo* antitumor potential of pyrimethamine was also evaluated in a SCID-mouse xenotransplantation model.

The agents that are commonly used against melanoma act by damaging cellular components to such an extent that apoptosis is induced (32). However, disseminated melanoma is largely resistant to conventional chemotherapeutic agents. The identification of different defects of the apoptosis program in melanoma cells suggests that multiple signaling pathways may need to be targeted for maximum therapeutic effectiveness.

Our data indicate that pyrimethamine induced apoptosis of melanoma cells via a mechanism, bringing into play both the caspase and cathepsin cascades. According to what was observed in activated lymphocytes (16), this effect did not require CD95/Fas engagement, as shown by experiments performed with a specific mAb blocking CD95/Fas. However, we cannot rule out the possibility that a ligand-independent aggregation of the death receptor and a recruitment of death-inducing signaling complex could occur, as shown with some oxidizing agents or bile acids (33, 34). Similarly to other antifolate compounds, pyrimethamine

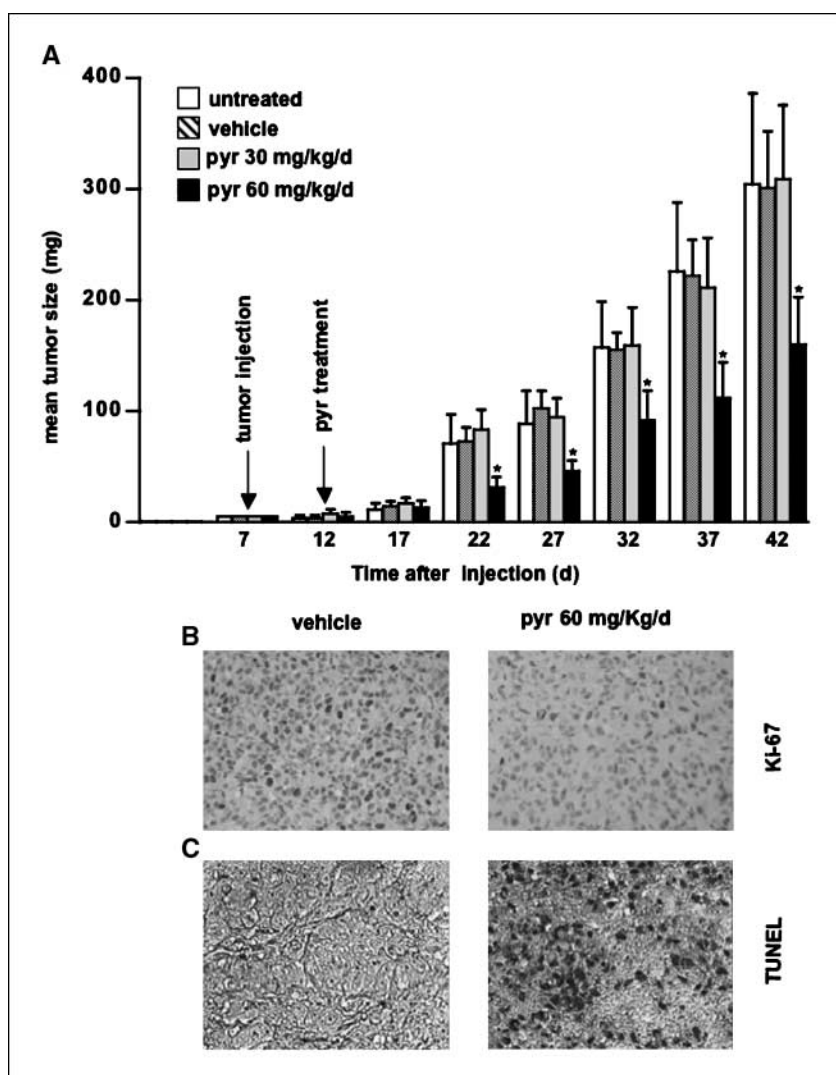


**Figure 6.** Effects of pyrimethamine on tumor growth, cell proliferation, and apoptosis in a SCID mouse model. **A**, tumor growth characteristics in SCID mice inoculated with the human melanoma cell line 501 and treated with vehicle alone or pyrimethamine. Pyrimethamine treatment (30 and 60 mg/kg once daily via gavage) was started at the onset of the metastatic tumor (i.e., 7 d after melanoma cell injection). *Columns*, mean of tumor weight at various times after melanoma cell injection; *bars*, SD. \*,  $P < 0.05$ , significance compared with untreated control mice. **B** and **C**, TUNEL staining of tumor sections from mice treated with vehicle alone (*left*) or 60 mg/kg/d of pyrimethamine (*right*). Morphometric analyses were performed on 20 microscope fields as described in Materials and Methods and indicated significant effects of pyrimethamine on both cell proliferation (i.e., Ki-67-positive cells) and apoptosis (i.e., TUNEL-positive cells).

induced mitochondrial depolarization, a late event in the mitochondrial driven apoptosis cascade (17). In this regard, it is interesting to consider that the expression of Bcl-2, a regulator of mitochondrial apoptotic activity, was down-regulated by pyrimethamine. Thus, pyrimethamine-induced apoptosis may be considered as a multifaceted process in which different inducers or regulators of apoptosis are simultaneously implicated, thus allowing death defects of melanoma cells to be overcome.

Cathepsin B seems to play a major role in the initiation of pyrimethamine-induced apoptotic pathway in the metastatic cell lines analyzed here. Under physiologic conditions, cathepsin B is localized within the lysosomes and is released into the cytoplasm upon stimulation or cell damage (8). Its release into the cytoplasm contributes to apoptosis execution. Different mechanisms that can contribute to lysosomal permeabilization, probably in a stimulus type-dependent and cell type-dependent fashion, have been described (30, 35). According to literature, one mechanism of pyrimethamine-induced lysosomal permeabilization could be the generation of reactive oxygen species (36).

The proteins that are cleaved by cathepsin B are not well defined (8). However, literature data suggest a target effect of cathepsin B on mitochondrial homeostasis with the activation of a mitochondrial-mediated apoptotic program (37). In fact, it has been shown that cathepsin B, once released into the cytoplasm, enhances both the mitochondrial release of cytochrome *c* and the subsequent activation of caspase-9 (37). According to this sequence, our data show an early release of cytochrome *c*, after pyrimethamine addition, followed by the activation of caspase-9, in both melanoma cell lines.

In the 501 cell line, another target for pyrimethamine could be the caspase-8-driven cascade. In fact, pyrimethamine was able to induce upstream caspase activation (caspase-8), bypassing CD95/Fas engagement, similarly to what we had previously observed in activated lymphocytes from a patient with a lymphoproliferative syndrome (16). This is noteworthy considering that the melanoma cell lines used in this study were shown to defy CD95-mediated apoptosis *in vitro*.

Briefly, our results suggest a key role for cathepsin B as an early inducer of pyrimethamine-induced apoptosis, whereas the contribution of caspases was detected later in both 501 and 8863 cell lines. The involvement of cathepsin and caspase activation in the pyrimethamine-dependent apoptotic pathway could be responsible for the slight inhibitory effect on drug-induced apoptosis exerted by the pan-caspase inhibitor Z-VAD-FMK and/or the cathepsin B inhibitor CA-074-Me when used alone, especially in the 501 cell line. In fact, the inhibition of one of the two pathways could boost the other one as was also suggested by the observation that the combined usage of the two inhibitors completely abrogated pyrimethamine-induced apoptosis. This effect could provide therapeutic benefits in melanoma cells by targeting different resistance mechanisms.

*In vivo* studies in SCID mice seem to be in line with *in vitro* studies. In fact, although monotherapy with pyrimethamine was only partially capable of impairing tumor growth, a significant effect of the drug in terms of antiproliferative and proapoptotic activities was observed. This indicates that further studies with combination protocols taking into account conventional chemotherapeutic agents and/or biological therapies (e.g., type I IFNs) are mandatory to assess the real antitumor potential of pyrimethamine.

Finally, there is increasing agreement that autophagy could represent a fruitful survival strategy for metastatic cancer cells (38). In particular, metastatic tumor cells are shown to be able not only to "recycle," by autophagic processes, degenerated organelles, or altered proteins (self cannibalism), but also to engulf and digest foreign material, including cell debris from necrotic cells, as well as apoptotic bodies or entire apoptosis-triggered cells (xeno-cannibalism; refs. 39, 40). This skill represents a formidable survival option for metastatic cells in adverse conditions, such as those they encounter in their "journey" toward the target organ to establish a colony. Hence, in line with the previously suggested activity of another widely used antifolate compound, i.e., methotrexate (41), the alterations we found after pyrimethamine treatment, i.e., the impairment of the lysosomal compartment activity and function and consequent cathepsin B release, could impair this key survival function and contribute to cell demise. In brief, pyrimethamine could damage autophagic processes, thus favoring cell deaths.

In conclusion, given the complex rewiring of cell death and survival pathways during melanomagenesis, it is unlikely that the cure for melanoma relies on a single agent. Most likely, effective treatments might include the combination of conventional chemotherapeutic and biological therapies aimed at targeting different resistance mechanisms. In this regard, pyrimethamine may be considered as an interesting candidate because it triggers different inducers or regulators of apoptosis, thus permitting death defects of melanoma cells to be overcome.

## Disclosure of Potential Conflicts of Interest

No potential conflicts of interest were disclosed.

## Acknowledgments

Received 1/17/2008; revised 4/2/2008; accepted 4/17/2008.

**Grant support:** Alleanza Contro il Cancro ACC3-ACC7 and Convenzione oncologica ordinaria IFO/ISS 32/07-Ministero della Sanità (W. Malorni).

The costs of publication of this article were defrayed in part by the payment of page charges. This article must therefore be hereby marked *advertisement* in accordance with 18 U.S.C. Section 1734 solely to indicate this fact.

We thank Claudia Travaglini (Department of Experimental Medicine, University of Rome "La Sapienza") for her excellent technical help; Dr. Fiorella Malchiodi-Albedi (Istituto Superiore di Sanità) for reagents and advice; and Roberta Terlizzi and Zaira Maroccia (Istituto Superiore di Sanità) for expert secretarial assistance.

## References

- Miller AJ, Mihm MC, Jr. Melanoma. *N Engl J Med* 2006; 355:51–65.
- Garbe C, Eigentler TK. Diagnosis and treatment of cutaneous melanoma: state of the art 2006. *Melanoma Res* 2007;17:117–27.
- Tarhini AA, Agarwala SS. Cutaneous melanoma: available therapy for metastatic disease. *Dermatol Ther* 2006;19:19–25.
- Kirkwood JM, Moschos S, Wang W. Strategies for the development of more effective adjuvant therapy of melanoma: current and future explorations of antibodies, cytokines, vaccines, and combinations. *Clin Cancer Res* 2006;12:2331–68.
- Soengas MS, Lowe SW. Apoptosis and melanoma chemoresistance. *Oncogene* 2003;22:3138–51.
- Hersey P. Apoptosis and melanoma: how new insights are effecting the development of new therapies for melanoma. *Curr Opin Oncol* 2006;18:189–96.
- Fulda S, Debatin KM. Extrinsic versus intrinsic apoptosis pathways in anticancer chemotherapy. *Oncogene* 2006;25:4798–811.
- Chwieralski CE, Welte T, Buhling F. Cathepsin-regulated apoptosis. *Apoptosis* 2006;11:143–9.
- Sloane BF, Rozhin J, Johnson K, Taylor H, Crissman JD, Honn KV. Cathepsin B: association with plasma membrane in metastatic tumors. *Proc Natl Acad Sci U S A* 1986;83:2483–7.
- Matarrese P, Di Biase L, Santodonato L, et al. Type I

- interferon gene transfer sensitizes melanoma cells to apoptosis via a target activity on mitochondrial function. *Am J Pathol* 2002;160:1507-20.
11. 1999 USPHS/IDSA guidelines for the prevention of opportunistic infections in persons infected with human immunodeficiency virus. *Clin Infect Dis* 2000;30:S29-65.
  12. Bygbjerg IC. Pyrimethamine-induced alterations in human lymphocytes *in vitro*. Mechanisms and reversal of the effect. *Acta Pathol Microbiol Immunol Scand* 1985;93:183-8.
  13. Bygbjerg IC, Odum N, Theander TG. Effect of pyrimethamine and sulphadoxine on human lymphocyte proliferation. *Trans R Soc Trop Med Hyg* 1986;80:295-300.
  14. Viora M, De Luca A, D'Ambrosio A, Antinori A, Ortona E. *In vitro* and *in vivo* immunomodulatory effects of anti-*Pneumocystis carinii* drugs. *Antimicrob Agents Chemother* 1996;40:1294-7.
  15. van der Werff Ten Bosch J, Schotte P, Ferster A, et al. Reversion of autoimmune lymphoproliferative syndrome with an antimalarial drug: preliminary results of a clinical cohort study and molecular observations. *Br J Haematol* 2002;117:176-88.
  16. Pierdominici M, Giammarioli AM, Gambardella L, et al. Pyrimethamine (2,4-diamino-5-p-chlorophenyl-6-ethylpyrimidine) induces apoptosis of freshly isolated human T lymphocytes, bypassing CD95/Fas molecule but involving its intrinsic pathway. *J Pharmacol Exp Ther* 2005;315:1046-57.
  17. Kroemer G, Zamzami N, Susin SA. Mitochondrial control of apoptosis. *Immunol Today* 1997;18:44-51.
  18. Lozupone F, Rivoltini L, Luciani F, et al. Adoptive transfer of an anti-MART-1(27-35)-specific CD8+ T cell clone leads to immunoselection of human melanoma antigen-loss variants in SCID mice. *Eur J Immunol* 2003;33:556-66.
  19. Cossarizza A, Franceschi C, Monti D, et al. Protective effect of N-acetylcysteine in tumor necrosis factor- $\alpha$ -induced apoptosis in U937 cells: the role of mitochondria. *Exp Cell Res* 1995;220:232-40.
  20. Ceruti S, Beltrami E, Matarrese P, et al. A key role for caspase-2 and caspase-3 in the apoptosis induced by 2-chloro-2'-deoxy-adenosine (cladribine) and 2-chloro-adenosine in human astrocytoma cells. *Mol Pharmacol* 2003;63:1437-47.
  21. Geran RI, Greenberg NH, Macdonald MM, Shumacher AM, Abbot BJ. Protocols for screening chemical agents and natural products against animal tumors and other biological systems. *Cancer Chemother Rep* 1972;3:1-88.
  22. Klinker H, Langmann P, Richter E. Plasma pyrimethamine concentrations during long-term treatment for cerebral toxoplasmosis in patients with AIDS. *Antimicrob Agents Chemother* 1996;40:1623-7.
  23. Qurt I, Verma S, Petrella T, Bak K, Charette M. Temozolomide for the treatment of metastatic melanoma: a systematic review. *Oncologist* 2007;12:1114-23.
  24. Brada M, Judson I, Beale P, et al. Phase I dose-escalation and pharmacokinetic study of temozolomide (SCH 52365) for refractory or relapsing malignancies. *Br J Cancer* 1999;81:1022-30.
  25. Strauss G, Osen W, Debatin KM. Induction of apoptosis and modulation of activation and effector function in T cells by immunosuppressive drugs. *Clin Exp Immunol* 2002;128:255-66.
  26. Lugini L, Lozupone F, Matarrese P, et al. Potent phagocytic activity discriminates metastatic and primary human malignant melanomas: a key role of ezrin. *Lab Invest* 2003;83:1555-67.
  27. Werneburg NW, Guicciardi ME, Bronk SF, Gores GJ. Tumor necrosis factor- $\alpha$ -associated lysosomal permeabilization is cathepsin B dependent. *Am J Physiol Gastrointest Liver Physiol* 2002;283:947-56.
  28. Perl A, Gergely P, Jr., Nagy G, Koncz A, Banki K. Mitochondrial hyperpolarization: a checkpoint of T-cell life, death and autoimmunity. *Trends Immunol* 2004;25:360-7.
  29. Matarrese P, Gambardella L, Cassone A, Vella S, Cauda R, Malorni W. Mitochondrial membrane hyperpolarization hijacks activated T lymphocytes toward the apoptotic-prone phenotype: homeostatic mechanisms of HIV protease inhibitors. *J Immunol* 2003;170:6006-15.
  30. Ferri KF, Kroemer G. Organelle-specific initiation of cell death pathways. *Nat Cell Biol* 2001;3:E255-63.
  31. Freund YR, Riccio ES, Phillips SJ, Dousman L, MacGregor JT. Pyrimethamine impairs host resistance to infection with *Listeria monocytogenes* in BALB/c mice. *Toxicol Sci* 1998;42:91-8.
  32. Hersey P, Zhuang L, Zhang XD. Current strategies in overcoming resistance of cancer cells to apoptosis melanoma as a model. *Int Rev Cytol* 2006;251:131-58.
  33. Graf D, Kurz AK, Fischer R, Reinehr R, Haussinger D. Taurolithocholic acid-3 sulfate induces CD95 trafficking and apoptosis in a c-Jun N-terminal kinase-dependent manner. *Gastroenterology* 2002;122:1411-27.
  34. Scheel-Toellner D, Wang K, Craddock R, et al. Reactive oxygen species limit neutrophil life span by activating death receptor signaling. *Blood* 2004;104:2557-64.
  35. Brunk UT, Neuzil J, Eaton JW. Lysosomal involvement in apoptosis. *Redox Rep* 2001;6:91-7.
  36. Jin S, White E. Role of autophagy in cancer: management of metabolic stress. *Autophagy* 2007;3:28-31.
  37. Guicciardi ME, Leist M, Gores GJ. Lysosomes in cell death. *Oncogene* 2004;23:2881-90.
  38. Hippert MM, O'Toole PS, Thorburn A. Autophagy in cancer: good, bad, or both? *Cancer Res* 2006;66:9349-51.
  39. Lugini L, Matarrese P, Tinari A, et al. Cannibalism of live lymphocytes by human metastatic but not primary melanoma cells. *Cancer Res* 2006;66:3629-38.
  40. Matarrese P, Ciarlo L, Tinari A, Piacentini M, Malorni W. Xeno-cannibalism as an exacerbation of self-cannibalism: a possible fruitful survival strategy for cancer cells. *Curr Pharm Des* 2008;14:245-52.
  41. Salvador N, Aguado C, Horst M, Knecht E. Import of a cytosolic protein into lysosomes by chaperone-mediated autophagy depends on its folding state. *J Biol Chem* 2000;275:27447-56.